ELSEVIER

Journal of Experimental Marine Biology and Ecology
281 (2002) 13–40

Journal of EXPERIMENTAL MARINE BIOLOGY AND ECOLOGY

www.elsevier.com/locate/jembe

A functional model of responsive suspension-feeding and growth in bivalve shellfish, configured and validated for the scallop *Chlamys farreri* during culture in China

A.J.S. Hawkins[a,*], P. Duarte[b], J.G. Fang[c], P.L. Pascoe[a], J.H. Zhang[c], X.L. Zhang[d], M.Y. Zhu[d]

[a] *Plymouth Marine Laboratory, Prospect Place, The Hoe, Plymouth PL1 3DH, UK*
[b] *University Fernando Pessoa, 349 Praça 9 de Abril, Porto 4249-004, Portugal*
[c] *Yellow Sea Fisheries Research Institute, 106 Nanjing Road, Qingdao 266071, PR China*
[d] *First Institute of Oceanography, State Oceanic Administration, 6 Xianxialing Road, Qingdao 266061, PR China*

Received 17 May 2002; received in revised form 24 August 2002; accepted 3 September 2002

Abstract

A dynamic growth model is presented for the suspension-feeding scallop *Chlamys farreri*. The model is configured and validated for *C. farreri* cultured in Sungo Bay, China, using functional relations to simulate rapid and sensitive adjustments in feeding and metabolism as observed in response to the highly changeable environment there. Notable novel elements include resolving significant adjustments in the relative processing of living chlorophyll-rich phytoplankton organics, non-phytoplankton organics and the remaining inorganic matter during both differential retention on the gill and selective pre-ingestive rejection within pseudofaeces. We also include a facility to predict the energy content of non-phytoplankton organics. This is significant, for living phytoplankton contributed less than 20% towards suspended particulate organic matter within Sungo Bay. Further, the energy content of non-phytoplankton organics was very much more variable than for phytoplankton organics. Whether using that facility or assuming an average value for the energy content of non-phytoplankton organics, resolution of the relative processing of different particle types allows simulation of how the rates, organic compositions and energy contents of filtered, ingested and deposited matter change in response to differences in seawater temperature, seston availability and seston composition. Dependent relations predict rates of energy absorption, energy expenditure and excretion. By these means, our model replicates dynamic adjustments in feeding and metabolism

* Corresponding author. Tel.: +44-1752-633100; fax: +44-1752-633101.
E-mail address: ajsh@pml.ac.uk (A.J.S. Hawkins).

PII: S0022-0981(02)00408-2

across full ranges of relevant natural variability, and successfully simulates scallop growth from larvae or seed to harvestable size under different temporal and spatial scenarios of culture. This is an important advance compared with simpler models that do simulate responsive adjustments. Only by modelling the complex set of feedbacks, both positive and negative, whereby suspension feeding shellfish interact with ecosystem processes, can one realistically hope to assess environmental capacities for culture.

Keywords: *Chlamys farreri*; Seston composition; Suspension feeding behaviour; Dynamic growth model; Shellfish aquaculture

1. Introduction

Shellfish aquaculture is among the fastest-growing of all food-producing sectors, with increasing pressure to model sustainable environmental capacities for culture (e.g. Raillard and Menésguen, 1994; Fang et al., 1996; Dowd, 1997; James and Ross, 1997; Bacher et al., 1998; Ferreira et al., 1998). Such modelling is complicated by observations that filter-feeding in shellfish is highly responsive to fluctuations in the quantity and quality of available food, as frequently occur in nearshore environments where most such aquaculture takes place (Smaal et al., 1986; Fegley et al., 1992; Cranford and Hargrave, 1994). In particular, rapid regulatory adjustments in feeding rate, as well as in the selection of different particle types during initial retention on the gills and/or pre-ingestive rejection as pseudo-faeces, are being established in an increasing variety of species (e.g. Hawkins et al., 1996, 1998a, 1999, 2001; Arifin and Bendell-Young, 1997; Cranford and Hill, 1999; Brillant and MacDonald, 2000; Pouvreau et al., 2000a; Ren et al., 2000; Wong and Cheung, 2001) (contra Jørgensen, 1996). These physiological adjustments affect growth of the individual. By influencing the relative biogeochemical fluxes of different particles and nutrients, they also affect ecosystem processes. To account for such consequences in variable environments, there has been a growing tendency towards dynamic simulations that use differential equations to define functional physiological responses to environmental change. In these simulations, responses are integrated to describe time-varying rates of feeding and metabolism as component processes in the prediction of individual growth, the individual being treated as an input–output system with size and energy content as state variables (e.g. Ross and Nisbet, 1990; Brylinski and Sephton, 1991; Powell et al., 1992; Van Haren and Kooijman, 1993; Raillard et al., 1993; Barillé et al., 1997; Campbell and Newell, 1998; Grant and Bacher, 1998; Scholten and Smaal, 1999; Pouvreau et al., 2000b; Solidoro et al., 2000; Ren and Ross, 2001).

Standardized comparisons of functional responses to environmental change are establishing subtle yet significant differences between the feeding behaviour of separate species (e.g. Hawkins et al., 1998a,b; Yukihira et al., 1998). Those differences reflect evolutionary adaptation to specific ecological niches, such as evidenced by the comparative ingestion and/or digestion of different particle types (e.g. Møhlenberg and Riisgård, 1978; Shumway et al., 1985, 1991; Ward and MacDonald, 1996; Bougrier et al., 1997; Hawkins et al., 1998a; Beninger et al., 1999). Nevertheless, the form and underlying functions of key relations appear similar between species (Hawkins et al., 1998a,b, 1999),

suggesting that a generic model structure may be developed that simulates feeding behaviour and growth from data describing the main environmental variables of food abundance, food composition, temperature and salinity. Parameters defining relations within this model structure will need to be established in different species, populations and locations (refer to Discussion). However, by including the capacity for functional relations identified over a range of species and environments, the model structure itself would prove highly adaptable. Towards that generic model structure, we present here a fully functional simulation in a new approach that (i) predicts the relative filtration, pre-ingestive rejection and ingestion of living phytoplankton organics, remaining non-phytoplankton organics (i.e. bacteria, detritus) and inorganic matter; and (ii) simulates excretion, growth and reproduction from the ingestion of those different particle types. The model is configured and validated for the scallop *Chlamys farreri* during culture in Sungo Bay, China. It includes novel interrelations determined there, whilst drawing upon generic relations that have previously been established in other species. *C. farreri* is one of the main shellfish species reared in China, Korea and Japan, where there has been especially rapid development of aquaculture (Guo et al., 1999). Separate papers describe how the model that we present here has been integrated with other hydrodynamic, biogeochemical and ecophysiological simulations as tools to help address the associated need to optimize sustainable culture practices on a variety of scales (Bacher et al., submitted for publication; Duarte et al., submitted for publication (a,b); Nunes et al., in press).

2. Methods

2.1. Environmental characterization at Sungo Bay

Between May 1999 and April 2000, monthly samples were collected from seven sites throughout Sungo Bay, Shandong Province, China (37.1°N, 122.5°E) (Fig. 1) for measures of surface seawater temperature (TEMP; °C), salinity (SAL; ‰) and seston availability determined as total particulate mass (TPM; mg l^{-1}), particulate organic mass (POM; mg l^{-1}), particulate inorganic mass (PIM; mg l^{-1}), particulate organic carbon (POC; mg l^{-1}) and chlorophyll *a* (CHL; μg l^{-1}). Seston availability was determined by filtering water samples through 47 mm GF/C filters that had previously been incinerated at 450 °C for 3 h and weighed, when TPM was defined as the weight-difference after drying the filter and sample at 60 °C for 24 h, PIM as the weight-difference after incinerating at 450 °C for 3 h, and POM as the difference between TPM and PIM. Chlorophyll *a* was measured in samples that had been collected on 25 mm GF/F filters using standard procedures for acetone extraction and fluorometric analysis (Holm-Hansen et al., 1965).

2.2. Ecophysiological experiments to define functional relations describing feeding behaviour

Suspension-feeding behaviour in the scallop *C. farreri* (Jones and Preston) was studied in response to natural and experimental variations in the amount and composition of suspended seston within Sungo Bay as described by Hawkins et al. (2001), and

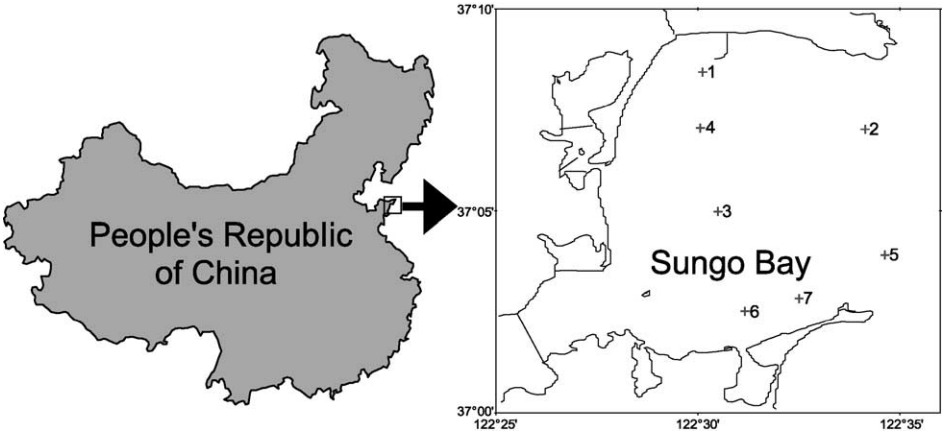

Fig. 1. Sampling sites in Sungo Bay.

associated measures of biodeposition used to calculate weight-standardized rates of filtration, pre-ingestive rejection and ingestion according to Hawkins et al. (1999). We also measured influences of both short-term and seasonal changes in seawater temperature on rates of feeding and metabolism as described by Zhang et al. (submitted for publication).

2.3. Model structure

STELLA® Research software (Version 6) (High Performance Systems, Hanover, USA), a graphical modelling package, was used to simulate mussel growth with a time step of 1 day. Variables and interrelations in the model are defined and illustrated in Table 1 and Fig. 2. In the following subsections, we include statistical validations of fitted relations from our associated experiments to define responses, including explanation as necessary to understand and substantiate our model structure.

2.3.1. Resolving particulate organic matter and energy contents

Phytoplankton organics (PHYORG; mg) were estimated according to Grant and Bacher (1998), multiplying measured chlorophyll *a* (CHL; mg) by 50 to give total phytoplankton organic carbon, based on values measured in nutrient-rich surface waters (Welschmeyer and Lorenzen, 1984; Taylor et al., 1997), and dividing that phytoplankton organic carbon by 0.38 to give PHYORG, where 0.38 represents an average conversion for natural algal blooms within nearshore waters (Platt and Irwin, 1973; Soletchnik et al., 1996). The amount of remaining non-phytoplankton organics (DETORG; mg l^{-1}) was then calculated as POM-PHYORG.

Whereas the energy content of phytoplankton organics was assumed to be 23.5 J mg^{-1} (Slobodkin and Richman, 1961), we demonstrate that the energy content of non-phytoplankton organics varied greatly between both sites and seasons (refer to Results). To account for this variability, we have included a facility in our model whereby if data are on hand describing the total particulate organic carbon (POC; μg l^{-1}) within available seston,

Table 1
Variables, relations and parameters used in the growth model

Forcing variables
TPM {mg l^{-1}}
POM {mg l^{-1}}
PIM {mg l^{-1}}
CHL {μg l^{-1}}
POC {μg l^{-1}}
Water temperature {°C}
Functions and parameters
Time
Day = if year < 1 then int(time) else int(time − 365 × (year − 1))
Year = (int(time/365) + 1)
Seston composition
OCS = POM/TPM {fraction}
PHYORG = CHL ÷ 1000 × 50/0.38 {mg l^{-1}}
DETORG = POM − PHYORG {mg l^{-1}}
EPOM = if POC>0 and POM>0 then (0.632+(0.086 × (POC ÷ (POM × 1000)) × 100)) × 4.187 else 0 {J mg^{-1}}
EDET = if EPOM>0 then ((POM × EPOM) − (PHYORG × 23.5)) ÷ DETORG else if POM>0 and POC = 0 then 6.1 else 0 {J mg^{-1}}
Temperature effects
Temperature effects on feeding=((234.7 ÷ (7.17 × (6.283)$^{0.5}$)) × exp(−0.5 × ((Water temperature − 22.2) ÷ 7.17)^2)) ÷ ((234.7 ÷ (7.17 × (6.283)$^{0.5}$)) × exp(−0.5 × ((12 − 22.2) ÷ 7.17)^2))
Temperature effects on maintenance = exp(0.074 × Water temperature) ÷ exp(0.074 × 15)
Allometry
Weight of a standard animal = 1 {g dry soft tissue}
Weight exponent for feeding = 0.62
Weight exponent for heat losses = 0.72
PHYORG processing
FRPHYORG = exp(7.5856+(18.11 × (log*N*(log*N*(POM + 3)))) +(−10.5 × (log*N*(POM + 3)))+(0.6919 × PHYORG)) × Temperature effects on feeding × ((Soft tissue weight/Weight of standard animal)$^{\text{Weight exponent for feeding}}$) × 24 {mg day^{-1}}
IRPHYORG = FRPHYORG − RRPHYORG {mg day^{-1}}
PHYCNFPOM = FRPHYORG ÷ FRPOM {fraction}
RRFRPHYORG = 1.0 − 0.895 × PHYCNFPOM {fraction}
RRPHYORG = FRPHYORG × RRFRPHYORG {mg day^{-1}}
DETORG processing
FRDETORG=(0.542 + 0.586 × DETORG) × Temperature effects on feeding × ((Soft tissue weight/Weight of standard animal)$^{\text{Weight exponent for feeding}}$) × 24 {mg day^{-1}}
FRPOM = FRDETORG + FRPHYORG {mg day^{-1}}
IRDETORG = FRDETORG − RRDETORG {mg day^{-1}}
RRDETORG = −0.00674 + 0.348 × FRDETORG {mg day^{-1}}
PIM processing
FRPIM = 19.06 × (1 − exp(−0.110 × (PIM − 1.87))) × Temperature effects on feeding × ((Soft tissue weight/Weight of standard animal)$^{\text{Weight exponent for feeding}}$) × 24 {mg day^{-1}}
IRPIM = FRPIM − RRPIM {mg day^{-1}}
RRPIM = −0.841 + 0.936 × FRPIM {mg day^{-1}}
TPM processing
FRTPM = FRPHY + FRPIM + FRDETORG {mg day^{-1}}

(continued on next page)

Table 1 (*continued*)

Functions and Parameters
IRTPM = FRTPM − RRTPM {mg day^{-1}}
RRTPM = RRDETORG + RRPHYORG + RRPIM {mg day^{-1}}
Post filtration selection efficiencies
DETSEING=(IRDETORG ÷ IRTPM) ÷ (FRDETORG ÷ FRTPM) {fraction}
PHYSEING=(IRPHYORG ÷ IRTPM) ÷ (FRPHYORG ÷ FRTPM) {fraction}
PIMSEING=(IRPIM/IRTPM) ÷ (FRPIM ÷ FRTPM) {fraction}
REPHY=(FRPHY ÷ FRTPM) ÷ (PHYORG ÷ TPM) {fraction}
Energy absorption
OCI=(IRPHYORG + IRDETORG) ÷ IRTPM {fraction}
NAEIO = 1.12 − 0.129 × 1 ÷ OCI {fraction}
NEA=((23.5 × IRPHYORG)+(EDET × IRDETORG)) × NAEIO {J day^{-1}}
Excretory losses
Weight standardized NEA=((Weight of standard animal ÷ Soft tissue weight)$^{\text{Weight exponent for feeding}}$) × NEA
O to N ratio = if (10 + 0.03636 × Weight standardized NEA)>50 then 50 else if (10 + 0.03636 × Weight standardized NEA) < 10 then 10 else (10 + 0.03636 × Weight standardized NEA) {ratio}
Excretory losses=(((Total heat losses ÷ 14.06)/16) ÷ O to N ratio) × 14 × 1000 {μg NH_4 day^{-1}}
Heat losses
Maintenance heat loss = 4.005 × 24 × Temperature effects on maintenance × (Soft tissue of standard animal)$^{\text{Weight exponent for heat losses}}$ {J day^{-1}}
Total heat losses = 0.23 × NEA + Maintenance heat loss {J day^{-1}}
Reproductive losses
Reproduction = if day = 165 then 0.07 × Soft tissue energy else if day = 250 then 0.04 × Soft tissue energy else 0 {J}
Net energy balance
NEB = NEA − Total heat losses − (Total excretory losses × 0.02428) {J day^{-1}}
State variables and associated derivations
Soft tissue energy
Soft tissue energy(t) = Soft tissue energy($t - dt$)+(Soft tissue energy increase − Spawning energy loss) × dt {J}
Initial Soft tissue energy = 2312 {J}
Soft tissue energy increase = if NEB>0 then if Soft tissue energy ÷ (Soft tissue energy + Shell energy) ≥ Energy ratio then 0.897 × NEB else NEB else 0 {J day^{-1}}
Spawning energy loss = if NEB < 0 then abs(NEB) + Reproduction else Reproduction {J day^{-1}}
Energy ratio = 0.897 {ratio between total soft tissue energy and the energy in soft tissue plus shell}
Soft tissue weight
Soft tissue weight(t) = Soft tissue weight($t - dt$)+(Soft tissue weight increase − Spawning weight loss) × dt {g}
Initial Soft tissue weight = 0.116 {g}
Soft tissue weight increase = Soft tissue energy increase ÷ Soft tissue energy to weight conversion ÷ 1000 {g day^{-1}}
Soft tissue energy to weight conversion = 20 {J mg^{-1}}
Spawning weight loss = Spawning energy loss ÷ Soft tissue energy to weight conversion ÷ 1000 {g day^{-1}}
Shell energy
Shell energy(t) = Shell energy($t - dt$)+(Shell energy increase) × dt {J}
Initial Shell energy = 265 {J}
Shell energy increase = if NEB>0 and Soft tissue energy ÷ (Soft tissue energy + Shell energy) ≥ Energy ratio then 0.103 × NEB else 0 {J day^{-1}}
Shell weight
Shell weight(t) = Shell weight($t - dt$)+(Shell weight increase) × dt {g}
Initial Shell weight = 0.903 {g}

Table 1 (*continued*)

State variables and associated derivations
Shell weight increase = Shell energy increase ÷ Shell energy to weight conversion ÷ 1000 {g day^{-1}}
Shell energy to weight conversion = 0.294 {J mg^{-1}}
Total dry weight
Total dry weight = Soft tissue weight + Shell weight {g}
Total wet weight
Total wet weight = 0.1318 × (Shell length)$^{2.9294}$ {g}
Shell length
Shell length = 2.589 × (Shell weight)$^{0.343}$ {cm}

Refer to Methods for the definition of acronyms and the explanation of relations. Initial values for each state variable represent *C. farreri* of 2.5 cm shell length. Information in braces denotes units.

then the energy content of total particulate organic matter (EPOM; J mg^{-1} POM) is calculated as:

$$\mathrm{EPOM} = [(0.632 + (0.086 \times (\mathrm{POC} \div (\mathrm{POM} \times 1000)) \times 100)) \times 4.187],$$

according to Platt and Irwin (1973), applying a conversion of 4.187 J cal^{-1}, and assuming 23.5 J mg^{-1} dry phytoplankton organics (Slobodkin and Richman, 1961) to derive the energy content of non-phytoplankton organics (EDET; J mg^{-1}) as:

$$\mathrm{EDET} = [(\mathrm{POM} \times \mathrm{EPOM}) - (\mathrm{PHYORG} \times 23.5)] \div \mathrm{DETORG}.$$

2.3.2. Filtration, rejection and ingestion rates

To account for responsive adjustments in both the selective retention and the selective pre-ingestive rejection of different particle types, the model uses relations derived from our experimental measures in Sungo Bay (refer to Section 2.2) to predict separate filtration and rejection rates for PHYORG, DETORG and PIM.

The relation that best described filtration of phytoplankton organics (FRPHYORG; mg h^{-1} g^{-1}) included a combination of gamma curve and linear equations as follows:

$$\mathrm{FRPHYORG} = \mathrm{e}^{(7.5856 + (18.11 \times (\log N(\log N(\mathrm{POM}+3)))) + (-10.5 \times (\log N(\mathrm{POM}+3))) + (0.6919 \times \mathrm{PHYORG}))},$$

where adjusted $r^2 = 0.64$, residual $df = 36$ and $p < 0.000001$.

The relation that best described filtration of non-phytoplankton organics (FRDETORG; mg h^{-1} g^{-1}) was a linear equation as follows:

$$\mathrm{FRDETORG} = 0.542 + (0.586 \times \mathrm{DETORG}),$$

where adjusted $r^2 = 0.66$, residual $df = 38$ and $p < 0.000001$.

The relation that best described filtration of inorganic matter (FRPIM; mg h^{-1} g^{-1}) FRPIM was an exponential equation as follows:

$$\mathrm{FRPIM} = 19.06(2.68) \times [1 - \mathrm{e}^{-0.110 \times (\mathrm{PIM} - 1.87)}],$$

where adjusted $r^2 = 0.58$, residual $df = 66$ and $p < 0.000001$.

Filtration of total particulate matter (FRTPM; mg h^{-1}) was calculated as FRTPM = FRPHYORG + FRDETORG + FRPIM.

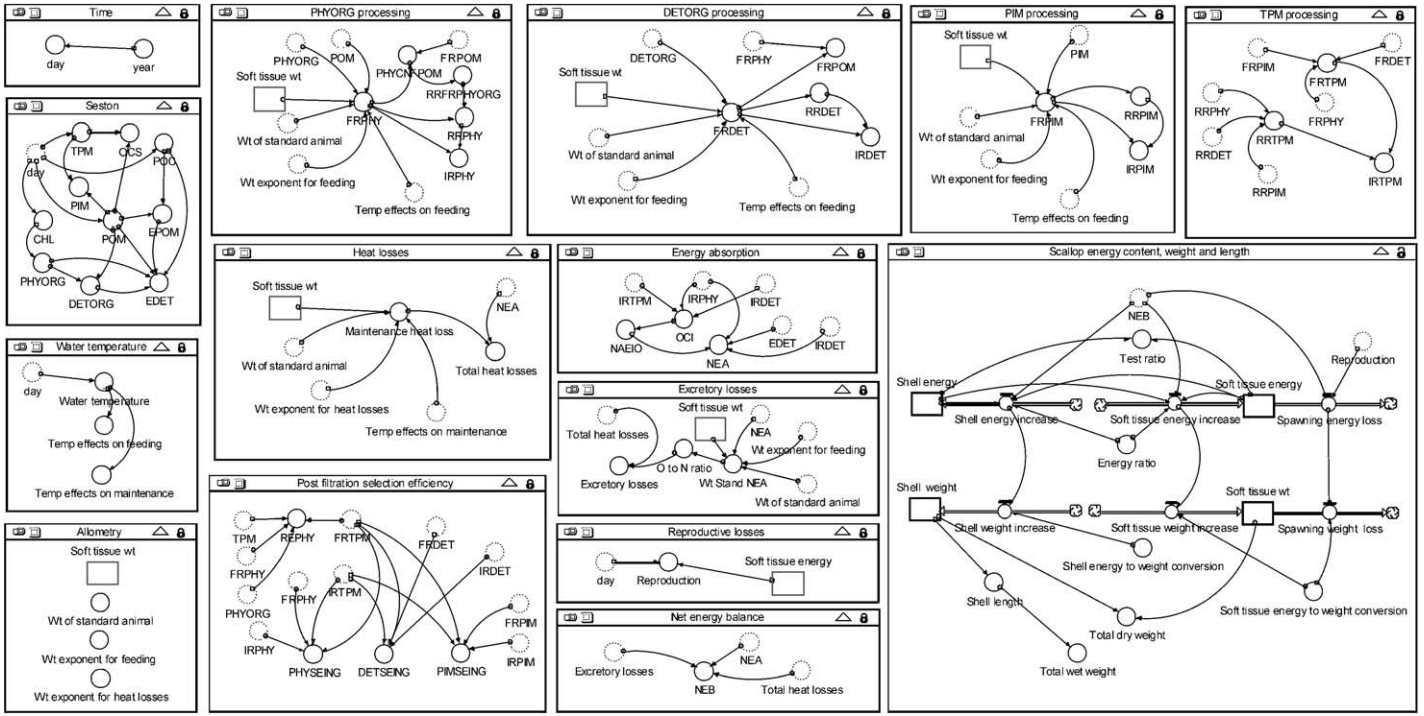

Fig. 2. Flow diagram of the growth model, illustrating main components using STELLA® Research software (High Performance Systems, Hanover, USA).

The best means of describing rejection of phytoplankton organics (RRPHYORG; mg h^{-1}) was first to simulate the proportion of filtered PHYORG that was rejected in pseudofaeces (RRFRPHYORG; fraction), according to an inverse relation with the proportion of phytoplankton organics within filtered POM (PHYCNFPOM; mg mg^{-1}) as follows:

$$\mathrm{RRFRPHYORG} = 1.0 - 0.895 \times \mathrm{PHYCNFPOM},$$

where PHYCNFPOM was calculated as PHYCNFPOM = FRPHYORG ÷ FRPOM, and where adjusted $r^2 = 0.69$, residual $df = 38$ and $p < 0.000001$.

RRPHYORG was then computed as RRPHY = RRFRPHYORG × FRPHY.

The relation that best described rejection of non-phytoplankton organics (RRDETORG; mg h^{-1} g^{-1}) was a linear equation as follows:

$$\mathrm{RRDETORG} = -0.00674 + (0.348 \times \mathrm{FRDETORG}),$$

where adjusted $r^2 = 0.88$, residual $df = 37$ and $p < 0.000001$.

The relation that best described rejection of inorganic matter (RRPIM; mg h^{-1} g^{-1}) was a linear equation as follows:

$$\mathrm{RRPIM} = -0.841 + (0.936 \times \mathrm{FRPIM}),$$

where adjusted $r^2 = 0.99$, residual $df = 65$ and $p < 0.000001$.

Rejection of total particulate matter (RRTPM; mg h^{-1} g^{-1}) was calculated as

$$\mathrm{RRTPM} = \mathrm{RRPHYORG} + \mathrm{RRDETORG} + \mathrm{RRPIM}.$$

Ingestion rates for phytoplankton organics (IRPHYORG; mg h^{-1} g^{-1}), non-phytoplankton organics (IRDETORG; mg h^{-1} g^{-1}), inorganic matter (IRPIM; mg h^{-1} g^{-1}) and total particulate matter (IRTPM; mg h^{-1} g^{-1}) were calculated as:

$$\mathrm{IRPHYORG} = \mathrm{FRPHYORG} - \mathrm{RRPHYORG},$$

$$\mathrm{IRDETORG} = \mathrm{FRDETORG} - \mathrm{RRDETORG},$$

$$\mathrm{IRPIM} = \mathrm{FRPIM} - \mathrm{RRPIM}, \quad \text{and}$$

$$\mathrm{IRTPM} = \mathrm{FRTPM} - \mathrm{RRTPM}.$$

2.3.3. Efficiencies of selective retention on the gills, including post-filtration selection prior to ingestion

The efficiency with which phytoplankton organics were selectively retained on the gills (REPHY; fraction) was computed as follows:

$$\mathrm{REPHY} = [(\mathrm{FRPHY} \div \mathrm{FRTPM}) \div (\mathrm{PHYORG} \div \mathrm{TPM})].$$

Efficiencies with which particles were selectively ingested, post-filtration, were computed for phytoplankton organics (PHYSEING; fraction), non-phytoplankton

organics (DETSEING; fraction) and inorganic matter (PIMSEING; fraction) as follows:

$$\text{PHYSEING} = [(\text{IRPHY} \div \text{IRTPM}) \div (\text{FRPHY} \div \text{FRTPM})],$$

$$\text{DETSEING} = [(\text{IRDET} \div \text{IRTPM}) \div (\text{FRDET} \div \text{FRTPM})], \quad \text{and}$$

$$\text{PIMSEING} = [(\text{IRPIM} \div \text{IRTPM}) \div (\text{FRPIM} \div \text{FRTPM})].$$

2.3.4. Absorption efficiency

The equation that best described net organic absorption efficiency (NAEIO; fraction) was an inverse relation with the organic content of ingested matter (OCI; fraction) as follows:

$$\text{NAEIO} = 1.12 + [-0.129 \times (1 \div \text{OCI})],$$

where OCI was calculated as [(IRPHYORG + IRDETORG) ÷ IRTPM], and where adjusted $r^2 = 0.89$, residual $df = 38$ and $p < 0.000001$.

This relation was statistically similar for different types of ingested organic matter, whether deriving from the natural seston, resuspended silt or cultured microalga used to manipulate dietary composition in our defining experiments ($p < 0.001$) (Hawkins et al., 2001). Similar relations have also been observed for different particle types in other shellfish species (e.g. Hawkins et al., 1998b, 1999), and is the main reason that we have modelled filtration, rejection and ingestion in terms of organic matter rather than carbon.

2.3.5. Energy absorption

Net energy absorption (NEA; J h^{-1}) was calculated as:

$$\text{NEA} = [(23.5 \times \text{IRPHYORG}) + (6.1 \times \text{IRDETORG})] \times \text{NAEIO},$$

where 1 mg^{-1} dry phytoplankton organics = 23.5 J (Slobodkin and Richman, 1961), and 6.1 J mg^{-1} non-phytoplankton organics is the annual average (± 2 S.E.) of 6.1 ± 1.4 measured throughout Sungo Bay (refer to Results), estimated on the basis of POC as described in Section 2.3.1 above. This seasonal and spatial average is similar to that of 6.3 J mg^{-1} calculated from proximate biochemical measures during March in the bay of Marennes Olèron, at a time when living phytoplankton organics comprised a negligible proportion of the total suspended particulate organic matter (Héral et al., 1983).

Alternatively, when able to use specific estimates of EDET on the basis of POC, NEA was calculated as:

$$\text{NEA} = [(23.5 \times \text{IRPHYORG}) + (\text{EDET} \times \text{IRDETORG})] \times \text{NAEIO}.$$

2.3.6. Heat losses

Using a calorimeter to measure total heat losses directly, it has been established that heat losses in excess of those under maintenance conditions of zero net energy balance were linearly related to energy intake as absorption increased across wide ranges in the

mussel *Mytilus edulis* and other animals (Hawkins et al., 1989; Widdows and Hawkins, 1989). Here, we have assumed values established in *M. edulis*, for which the energy costs of maintenance were 4.005 J h^{-1} g^{-1}, and total heat losses (THL; J h^{-1}) predicted as:

$$\mathrm{THL} = 4.005 + (0.23 \times \mathrm{NEA}),$$

where losses of 0.23 × NEA represent additional costs of feeding and growth.

2.3.7. Excretory losses

Excretory losses as ammonium were calculated from atomic ratios of oxygen consumed to nitrogen excreted (O:N ratio), calculated as $[(\mathrm{mg\ O_2}) \div 16] \div [(\mathrm{mg\ NH_4}) \div 14]$. Those O:N ratios were predicted on the basis of past studies showing general positive relations whereby starvation or low ration levels were associated with small ratios, but which increased at higher rations (e.g. Widdows, 1978; Epp et al., 1988). Published data describing oxygen consumption and ammonium excretion in *C. farreri* of 1-g soft dry tissue indicate that O:N ratios may range from a minimum of 10 to a maximum of about 50 (Lu et al., 2000). We have assumed that the O:N ratio increased linearly from 10 to 50 as weight standardized NEA ranged from 0 to 1100 J day^{-1} g^{-1} dry soft tissue, which represents a daily intake of about 5.5% of the soft tissue energy content, and is slightly above the maximum that we observed throughout our own experiments (refer to Section 2.2 above). On this basis, O:N ratio was predicted as:

$$\mathrm{O{:}N} = 10 + (0.03636 \times \text{weight standardized NEA}),$$

giving a minimum of 10 and maximum of 50 when weight standardized NEA is zero and 1100, respectively.

Excretory losses (EL; μg NH_4 h^{-1}) were then simulated as:

$$\mathrm{EL} = (((\mathrm{THL} \div 14.06) \div 16) \div \mathrm{O{:}N}) \times 14 \times 1000,$$

where 1 mg O_2 = 14.06 J (Gnaiger, 1983).

2.3.8. Energy balance

Net energy balance (NEB; J day^{-1}) was computed as:

$$\mathrm{NEB} = \mathrm{NEA} - \mathrm{THL} - (\mathrm{EL} \times 0.02428),$$

where 1 μg NH_4 = 0.02428 J (Elliot and Davison, 1975).

2.3.9. Reproductive losses

Spawning was set to occur as fixed proportions of 7% and 4% of total soft tissue energy contents during June and September, as reported for *C. farreri* whilst being ongrown during culture in Chinese waters (Lou, 1991). It was not necessary to invoke a more mechanistic prediction based upon gonad indices or biochemical status, for this level of spawning had a very small impact on annual growth. Indeed, the proportion of total soft tissue growth that was released as gametes during this first year of maturity under the current post-1999 culture scenario (refer to Section 2.5 below) was less than 3%, as is consistent with findings from other *Chlamys* species (MacDonald et al., 1991).

2.3.10. Shell and tissue growth

To establish the relative balance between energy deposited as soft tissue or shell, we assumed 19 122 J g^{-1} dry shell organic matter, averaged from three shellfish species (Cameron et al., 1979), and 1.54% organic content of dry shell, averaged from two scallop species (Price et al., 1976). The total energy content of *Chlamys* shell was therefore predicted to be $1 \times 0.0154 \times 19\,122 = 294$ J $g^{-1} = 0.294$ J mg^{-1} total dry shell weight. We also assumed 20 J mg^{-1} dry soft tissue (MacDonald et al., 1991). Applying these conversions to actual measures of growth as *C. farreri* increased from about 1- to 7-cm shell height in Sungo Bay (refer to Section 2.4 below), a strong linear relation was evident between soft tissue energy (SE; J) and total soft tissue plus shell energy (TE; J) as follows:

$$SE = 0.897 \times TE,$$

where adjusted $r^2 = 0.99$, residual $df = 131$ and $p < 0.000001$.

To maintain this balance between soft tissue and shell following periodic loss of soft tissues through spawning, growth in total soft tissues (TG; J day^{-1}) was predicted as:

$$TG = 0.897 \times NEB,$$

and growth in shell (SG; J day^{-1}) as:

$$SG = 0.103 \times NEB,$$

but only if the ratio of soft tissue energy to total soft tissue plus shell energy exceeded or equaled 0.897. Otherwise, all available energy was directed towards soft tissue growth.

Conversion to weight equivalents was effected using 0.294 J mg^{-1} dry shell and 20 J mg^{-1} dry soft tissue as justified above.

Conversion to shell length was effected using an allometric relation established from our measures of actual growth in Sungo Bay (refer to Section 2.4 below) whereby shell length (SL; cm) varied in strong positive relation with dry shell weight (SW; g) as follows:

$$SL = 2.589 \times SW^{0.343},$$

where adjusted $r^2 = 0.97$, residual $df = 131$ and $p < 0.000001$.

2.3.11. Effects of seawater temperature

Correction factors were applied that simulated effects of seasonal changes in seawater temperature upon filtration rates and maintenance heat losses. This was not necessary for rejection rates, ingestion rates and absorption rates; nor for the additional energy losses associated with growth over and above maintenance, which all depended upon filtration rate.

The correction factor describing temperature effects on filtration rate (TEF; fraction) was derived from a Gaussian curve that best described how clearance rate (CR; l h^{-1} g^{-1}) in *C. farreri* that had been fully acclimated under standardized conditions of food availability varied with natural seasonal changes in temperature (T; °C) (Zhang et al., submitted for publication) as follows:

$$CR = (233.9 \div (7.174 \times (6.283)^{0.5})) \times \exp(-0.5 \times ((T - 2.214) \div 7.174)^2),$$

where adjusted $r^2 = 0.85$, residual $df = 9$ and $p < 0.000001$.

On the basis of this curve, TEF was computed as:

$$\mathrm{TEF} = (234.7 \div (7.174 \times (6.283)^{0.5})) \times \exp(-0.5 \times ((-2.214) \div 7.174)^2) \div (234.7 \div (7.174 \times (6.283)^{0.5})) \times \exp(-0.5 \times ((12 - 22.214) \div 7.174)^2),$$

where relations describing filtration in the present model were derived from experimental measures when seawater in Sungo Bay was at 12 °C (Hawkins et al., 2001).

The correction factor describing temperature effects on maintenance heat losses (TEM; fraction) was derived assuming that TEM increased continually in logarithmic relation with seawater temperature according to a standard Q_{10} value of 2.1 as established in *C. farreri* and other species (e.g. Widdows, 1973; Bayne and Newell, 1983; Lu et al., 2000; Zhang et al., submitted for publication). On this basis, TEM was computed as:

$$\mathrm{TEM} = \exp(0.074 \times T) \div \exp(0.074 \times 15),$$

where energy costs of maintenance had been measured at 15 °C (refer to Section 2.3.6 above) (Hawkins et al., 1989).

2.3.12. Effects of scallop size

Relations described above that predict filtration responses, including the value of 4.005 J h^{-1} for energy costs of maintenance, were all standardized for an equivalent scallop of 1 g dry soft tissue weight. Corrections were effected using the formulation $Y_s=(W_s/W_e)^b \times Y_e$, where Y_s is the standardised parameter, W_s is the standard weight (1 g), W_e is the weight of experimental animal, Y_e is the uncorrected parameter, and b is the associated weight exponent. An exponent of 0.62 was used for FRPHYORG, FRDETORG and FRPIM (Hawkins et al., 2001). For maintenance heat losses, we used an exponent of 0.72 according to theoretical expectations for metabolism, as has been confirmed for oxygen consumption in *C. farreri* (Lu et al., 2000; Zhang et al., submitted for publication).

2.4. Field observations of actual growth

Average growth rates of cultured *C. farreri* were recorded monthly under normal nursery and rearing conditions at a hatchery, in a nursery area and on long lines that were all close to the shore near Site 2.

2.5. Simulations

Simulations were undertaken for two different culture scenarios as follows:

Traditional pre-1999 scenario: Commercial seeds from hatcheries that had set between late May and early July would be put in lantern nets sized about 1-cm shell length in October and maintained in nursery areas over the winter until the following April to mid-May when, at about 2-cm shell length, they were hung offshore on long lines. This usually enabled them to reach a market size of more than 6 cm from the following October onwards.

Current post-1999 scenario: This scenario was adopted in response to high and widespread mortalities that regularly occur during August and September (Zhang and

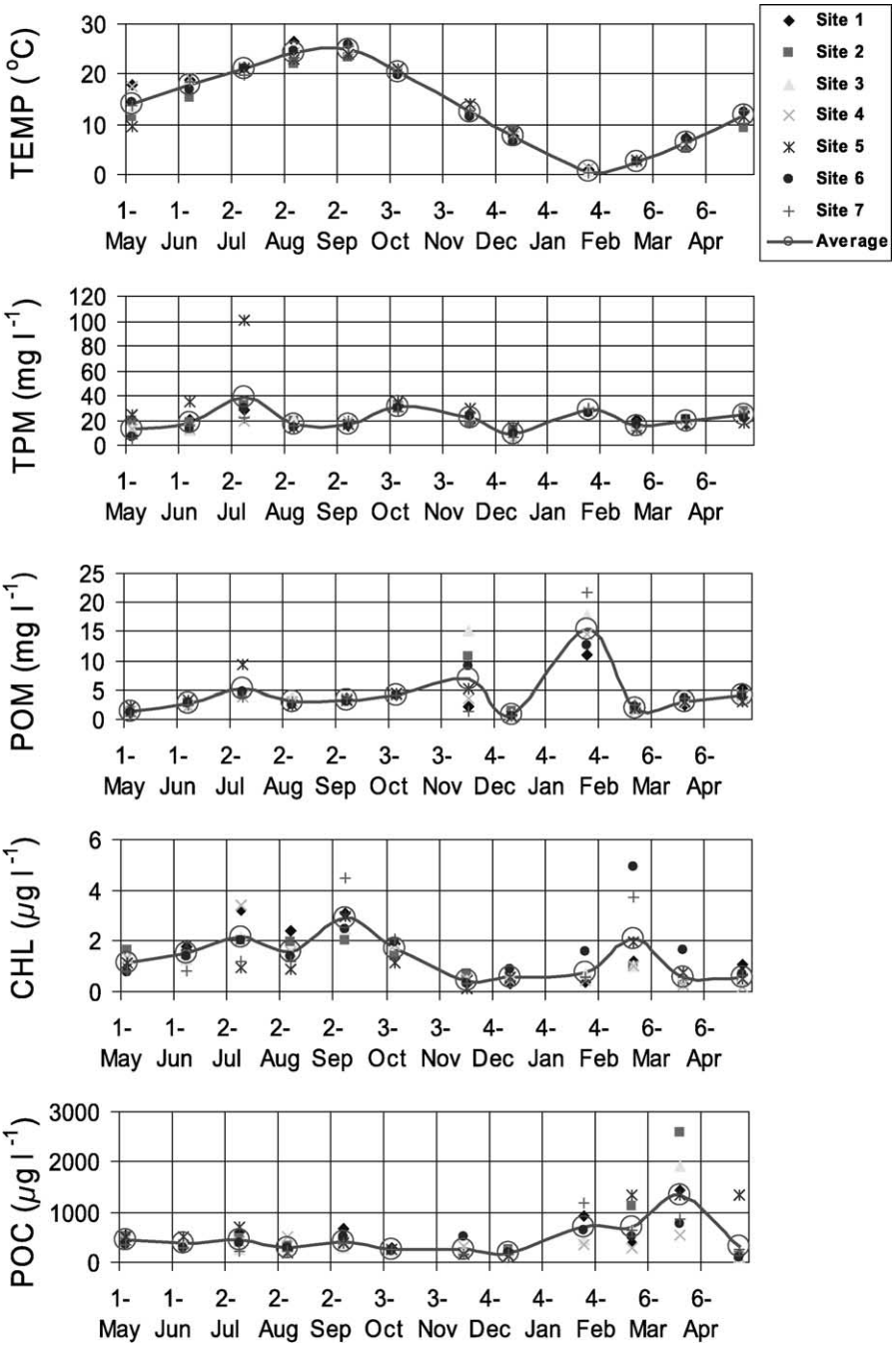

Fig. 3. Environmental characteristics in Sungo Bay: temperature (TEMP; °C), total particulate matter (TPM; mg l^{-1}), particulate organic matter (POM; mg l^{-1}), chlorophyll (CHL; µg l^{-1}) and particulate organic carbon (POC; µg l^{-1}) were measured monthly at each of seven sites illustrated in Fig. 1.

Yang, 1999), at the time of highest seawater temperatures (Fig. 3). To avoid those mortalities, *C. farreri* are now being bred later in the year, hung in lantern nets when about 2.5-cm shell length from mid-October to mid-November, and reared on long lines through the winter. This enables them to reach a reduced market size of more than 5 cm for harvest during the following June and July.

2.6. Sensitivity analysis

To establish the relative effects of each model parameter on model output, a single parameter was changed by either plus or minus 10% for each run of the model, requiring two runs per parameter, and the average percentage change in dry soft tissue weight resulting from that increase and decrease used as a measure of model sensitivity to that parameter. All analyses were undertaken for the present-day post-1999 scenario using average measures of TEMP, TPM, CHL and POM for all seven field sites, starting with a scallop of 2.5-cm shell length from 13th October, and running until July 31st.

3. Results

3.1. Seasonal changes in temperature, seston availability and seston composition

Seasonal changes in seawater temperature, seston availability and seston composition are illustrated at each of the seven sampling sites in Figs. 3 and 4. Seston availability over the year varied by an order of magnitude, and by a factor of up to about 5 between sites (Fig. 3). Non-phytoplankton organics (DETORG; mg l^{-1}) comprised more that 80% of POM at all sites throughout the year (Fig. 4). The energy content of non-phytoplankton organics (EDET; J mg^{-1}) was highly variable; average values at each site throughout the bay ranged from about 1 J mg^{-1} in October to about 16 J mg^{-1} in March (Fig. 4), with a seasonal average ($\pm$ 2 S.E.) for all sites of 6.1 $\pm$ 1.4 J mg^{-1}. Associated proportions that non-phytoplankton organics represented of the total seston energy content (DETE; fraction) were at seasonal minima of just above 50% in September and October, compared with maxima of about 97% in March (Fig. 4).

3.2. Simulated feeding and growth

Under the traditional pre-1999 scenario of seeding and harvest times, simulated growth of *C. farreri* grown from seed in lanterns on long lines approximated that expected. Whether simulated using the average POM or average POC measured at all sites through Sungo Bay, predicted shell length increased from 2 cm in April to reach marketable sizes of more than 6 cm during the following October, according to historical practice and records (Fig. 5).

Under the current post-1999 scenario of seeding and harvest times, simulated growth of *C. farreri* grown from spat to seed also approximated that expected. Whether simulated using the average POM or average POC measured at all sites through Sungo Bay,

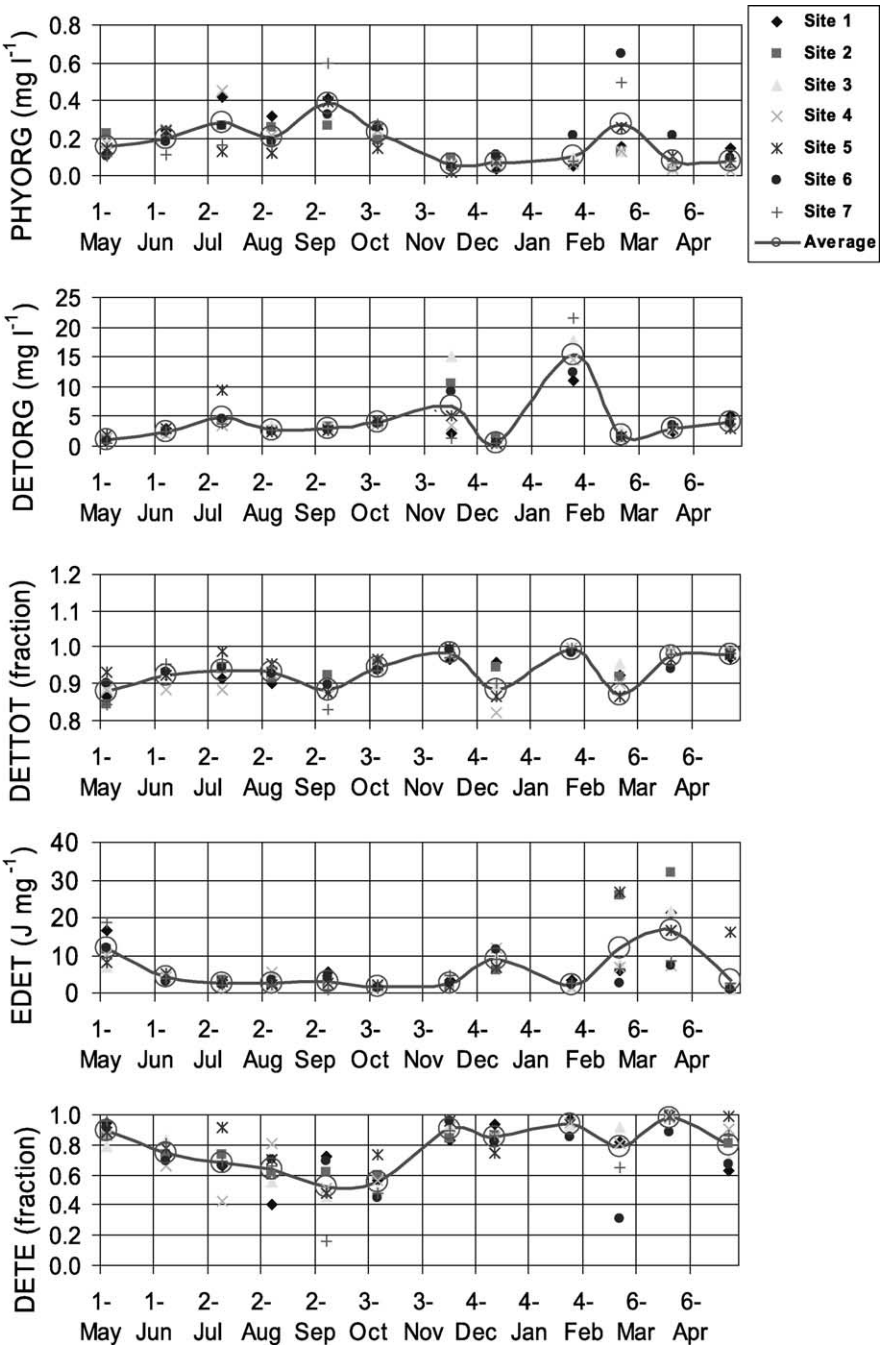
PHYORG (mg l-1)
DETORG (mg l-1)
DETTOT (fraction)
EDET (J mg-1)
DETE (fraction)
1- May
1- Jun
2- Jul
2- Aug
2- Sep
3- Oct
3- Nov
4- Dec
4- Jan
4- Feb
6- Mar
6- Apr
Site 1
Site 2
Site 3
Site 4
Site 5
Site 6
Site 7
Average

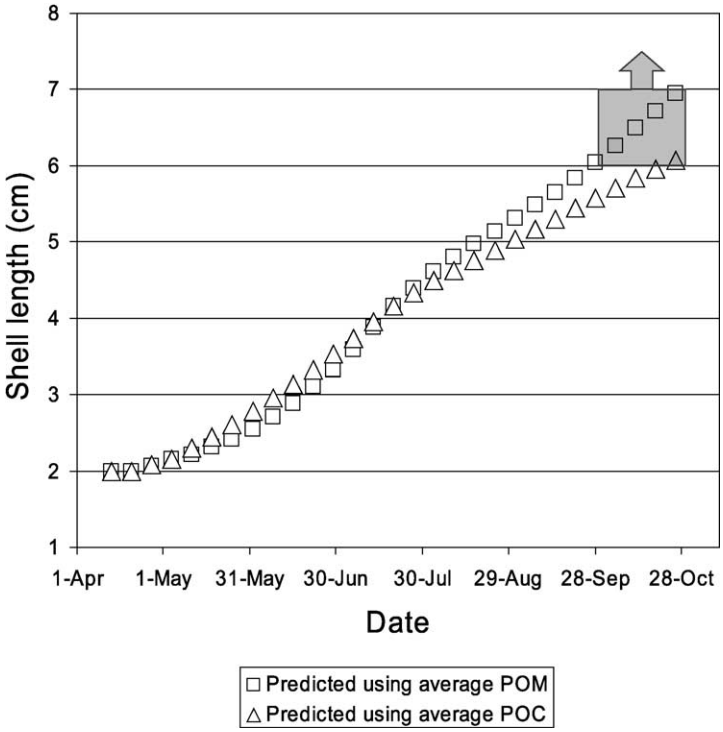

Fig. 5. *C. farreri* cultured in Sungo Bay: comparison of simulated and observed growth from seed to market-size, for traditional pre-1999 scenario of seeding and harvest times. Simulated growth is predicted from average environmental conditions recorded throughout the bay, and separate predictions illustrated here that are based upon organic availabilities measured as either POM or POC. The shaded box denotes ranges of normal shell length and dates upon harvest (6 to 7 cm harvested during October; refer to Methods).

predicted shell length increased from 3-mm shell length in July to between 2 and 3 cm during the following September, ready for putting into lantern nets under current practice (Fig. 6).

Also under the current post-1999 scenario, simulated growth of *C. farreri* grown from seed in lanterns on long lines again approximated that expected. Whether predicted from POM or from POC at each of the seven sites throughout Sungo Bay, shell length reached

Fig. 4. Environmental characteristics in Sungo Bay: living phytoplankton organics (PHYORG; mg l^{-1}), remaining detrital and bacterial organics (DETORG; mg l^{-1}), the proportion that DETORG comprised of POM (DETTOT; fraction), the energy content of DETORG (EDET; J mg^{-1}) and the proportion that energy within DETORG comprised of total seston energy content (DETE; fraction) were computed from characteristics illustrated in Fig. 3 for each of seven sites illustrated in Fig. 1. Calculations of PHYORG, DETORG and EDET are described in Methods. DETTOT was computed as (DETORG ÷ (PHYORG + DETORG)), and DETE as (EDET ÷ EPOM), where EPOM is the energy content of total suspended particulates (J mg^{-1}), calculated as described in Methods.

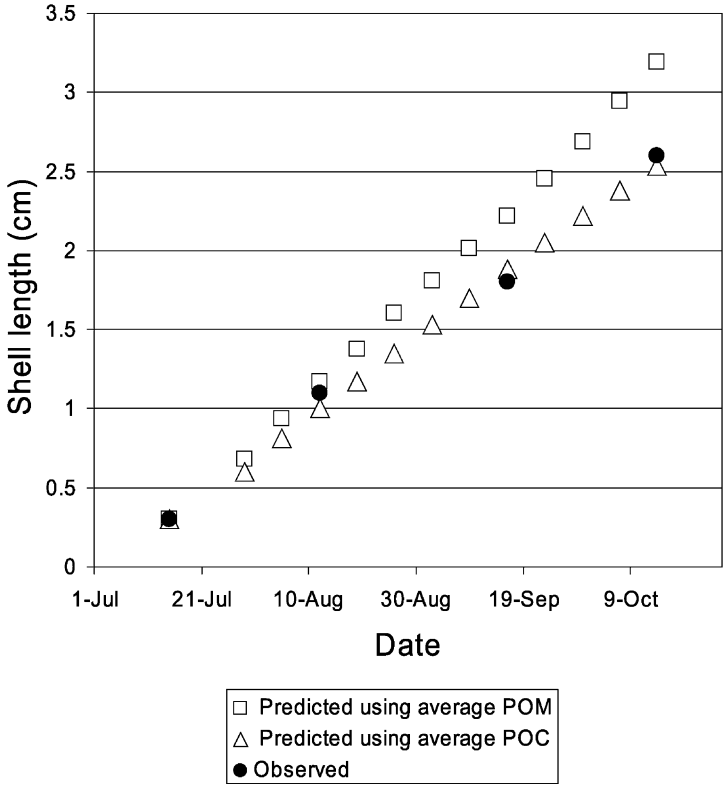

Fig. 6. *C. farreri* cultured in Sungo Bay: comparisons of simulated and observed growth from spat to seed, for the current post-1999 scenario of seeding and harvest times. Simulated growth is predicted from average environmental conditions recorded throughout the bay, and separate predictions illustrated here that are based upon organic availabilities measured as either POM or POC.

the expected minimum marketable size slightly before or during the normal time of harvest through June and July (Fig. 7a and b, respectively).

Relative to simulations based upon POM, those based upon POC predicted slower growth at each site during October and November (Fig. 7a and b, respectively). This was when values of EDET were consistently less than the value of 6.1 J assumed in predictions based upon POM alone, as the seasonal average mg^{-1} for all sites through the bay (refer to Methods) (Fig. 4).

Alternatively, following the winter months, growth predicted on the basis of POC started a month earlier than when simulated on the basis of POM; in March relative to April, respectively (Fig. 7a and b). This was when values of EDET were consistently higher than the seasonal average of 6.1 J mg^{-1} for all sites through the bay (Fig. 4).

Large differences in growth were predicted between sites, with fastest growth predicted at Site 3 in November and at Site 5 in July and August. These differences were mainly due to variation in the relative abundances of non-phytoplankton organics, which were highest at those same sites at times of fastest growth (Fig. 7a and b).

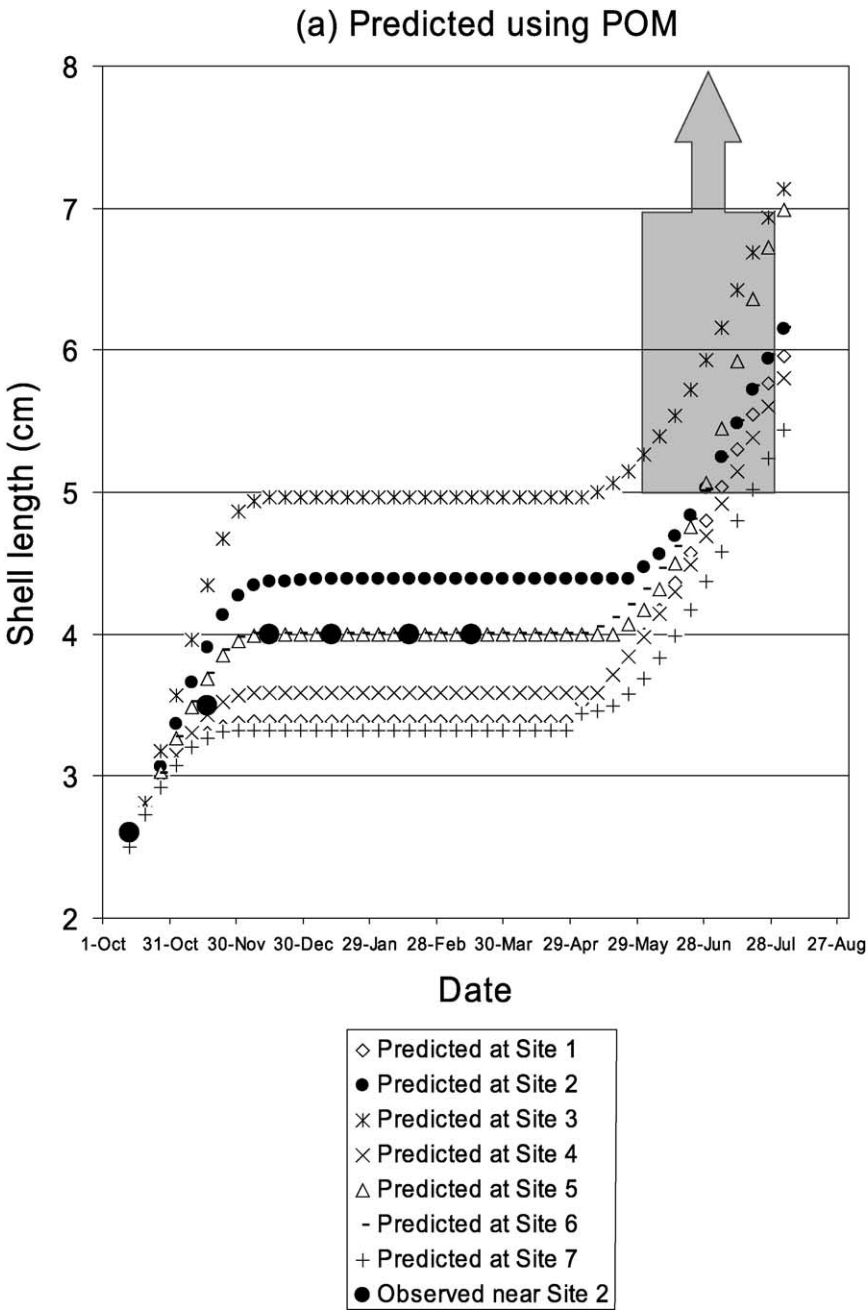

Fig. 7. *C. farreri* cultured in Sungo Bay: comparison of simulated and observed growth from seed to market-size, for the current post-1999 scenario of seeding and harvest times. Growth is simulated at each of seven sites throughout the Bay (refer to Fig. 1), and separate predictions illustrated here that are based upon organic availabilities measured as either (a) POM or (b) POC. Large filled circles illustrate growth observed near Site 2. The shaded boxes denote ranges of normal dates and shell length upon harvest (5 to 7 cm harvested during June and July; refer to Methods).

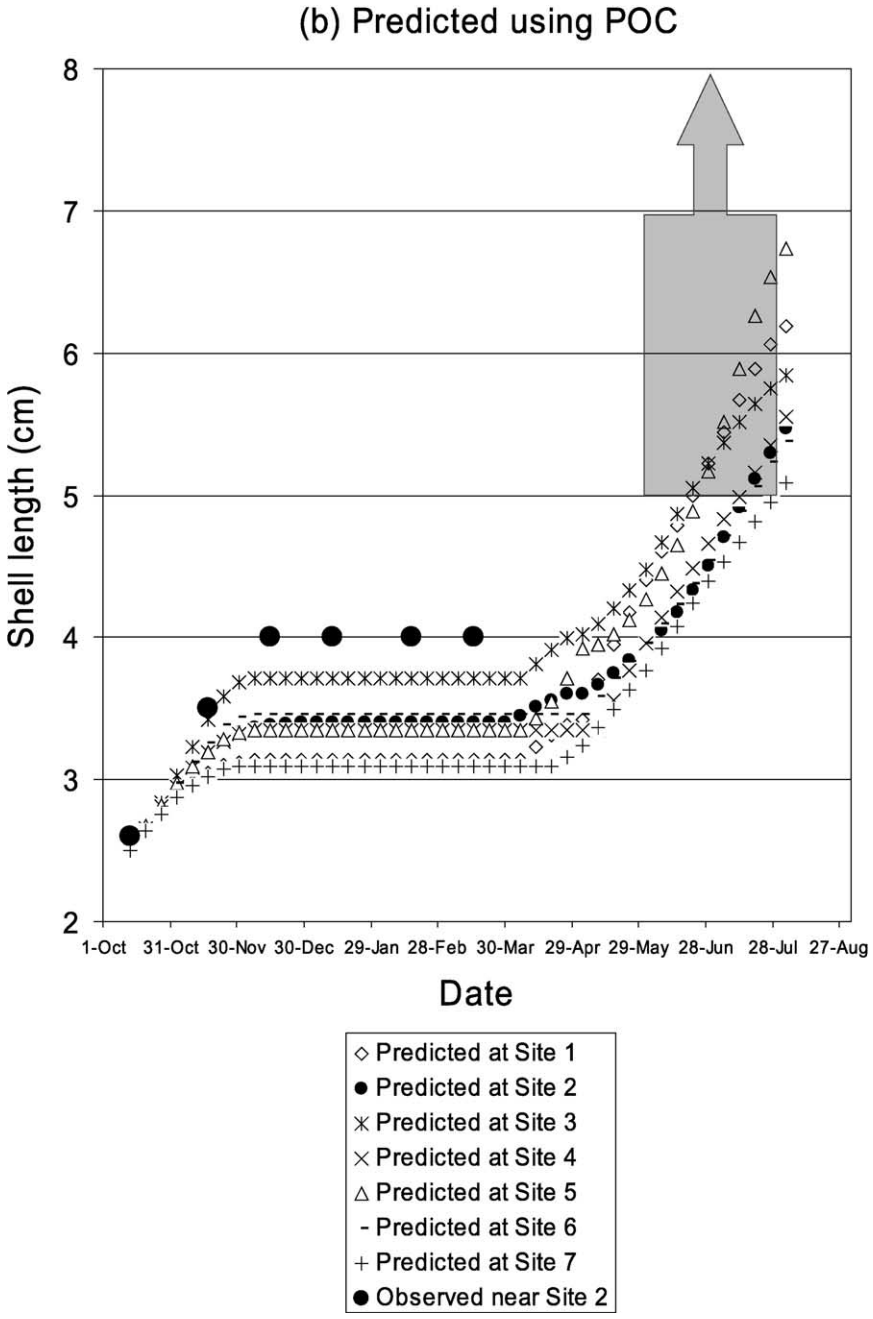

Fig. 7 (*continued*).

Table 2
Sensitivity analyses for model parameters, compared as the average percentage change in dry soft tissue weight resulting from adjustments of plus and minus 10% in each parameter (refer to Methods)

Model parameter	Parameter value	Percentage change in soft tissue weight		
		Plus 10% in parameter	Minus 10% in parameter	Average of each 10% adjustment
(1) Ratio of chlorophyll to carbon	50	3	3	3
(2) Ratio of carbon to organic matter	0.38	3	3	3
(3) Phytoplankton organics energy content	23.5 J mg^{-1}	3	4	4
(4) Weight exponent for feeding processes	0.62	12	13	13
(5) Weight exponent for maintenance respiration	0.72	6	5	6
(6) Maintenance respiration	4.005 J h^{-1} g^{-1}	9	9	9
(7) Heat loss per unit energy absorption above maintenance	0.23 J J^{-1}	8	7	7
(8) Maximum O:N ratio	50	1	1	1
(9) Fraction of NEB deposited as soft tissue	0.897	1	15	8
(10) Soft tissue energy content	20 J mg – 1	17	13	15
(11) Reproductive effort each seasonal spawning	0.07, 0.04	0	0.8	0.4

3.3. Sensitivity analyses

Average changes in dry soft tissue weight resulting from adjustments of plus and minus 10% in each model parameter are summarized in Table 2. Those changes were all less than 15%, indicating that predicted growth was relatively insensitive to those parameters, and that the model represents a robust simulation of scallop growth in Sungo Bay.

4. Discussion

Our model successfully simulates scallop growth from larvae or seed to harvestable size under different temporal and spatial scenarios of culture in the changeable environment of Sungo Bay. To achieve this, the model is highly dynamic, integrating key functional relations to simulate rapid and sensitive adjustments in feeding and metabolism that occur in response to frequent fluctuations in seawater temperature, seston availability and seston composition.

Functional models of this type depend on identifying the correct interrelations. The accuracy of our simulations under different spatial and temporal scenarios, together with the observation that predictions were relatively insensitive to our model parameters, suggests that we are some way down that road, and that the model is reasonably robust. Of particular importance is the question of how to define both food availability and food quality in terms that relate to feeding behaviour and other adaptations in the species of interest. Shellfish may selectively ingest and/or digest different particle types (e.g. Baker et al., 1998; Pouvreau et al., 2000a; Dupuy et al., 2000; Loret et al., 2000; Urrutia et al.,

2001; refer to Introduction), whilst effecting compensatory adjustments that may help to maximize the utilization of particles rich in chlorophyll (Hawkins et al., 1999, 2001). To account for these capabilities, our model resolves separate processing of the organic matter within living phytoplankton, remaining non-phytoplankton organics (i.e. bacteria, protozoans, colloids and detritus) and inorganic matter. For each of these dietary components, a separate functional relation simulates filtration, pre-ingestive rejection and ingestion, based solely upon data describing TPM, POM, PIM, CHL and TEMP. Using this approach, we can calculate the fractional organic content of ingested matter, and predict absorption efficiency on the basis of that organic content using an inverse relation that, to date, has appeared independent of dietary composition (refer to Methods). This important relation is the main reason that we have modeled filtration, rejection and ingestion in terms of organic matter, rather than carbon. By these means, our model is able to simulate feeding and growth over a broad range of environmental circumstances, whether in response to short-term tidal influences, seasonal effects or spatial differences. In contrast, many earlier models did not resolve any differential filtration of separate dietary components (e.g. Van Haren and Kooijman, 1993; Ross and Nisbet, 1990; Brylinski and Sephton, 1991; Powell et al., 1992; Barillé et al., 1997; Scholten and Smaal, 1999; Solidoro et al., 2000). Others, whilst resolving living phytoplankton from remaining organics, were without functional relations to simulate the highly responsive processes of selection and absorption, instead assuming a zero or constant percentage selection for chlorophyll-rich organics, and/or constant absorption efficiencies (e.g. Raillard et al., 1993; Campbell and Newell, 1998; Grant and Bacher, 1998; Pouvreau et al., 2000b; Ren and Ross, 2001).

Resolution of organic matter was achieved by predicting living phytoplankton organics (PHYORG; mg l^{-1}) on the basis of measured CHL, and deriving remaining organics (DETORG; mg l^{-1}) as the difference from POM. Whilst the energy content of living phytoplankton organics is known to fall within a small range (Slobodkin and Richman, 1961), that for remaining organics (EDET; J mg^{-1}) varies greatly according to composition. Therefore, where data for POC are available, we have included a novel facility to compute EDET, rather than assume an average value as is required in the absence of POC data (refer to Methods). This facility predicts a wide seasonal range for EDET (Fig. 4), and which was consistent with previous findings based upon proximate biochemical composition in the Bay of Marennes Olèron, France (Héral et al., 1983). Our findings also indicate that DETORG always represented more than 80% of POM, including more than 50% of all energy within the available seston (Fig. 4). Given the established ability of bivalve shellfish to digest and absorb non-phytoplankton organics (refer to Methods) (e.g. Williams, 1981; Kreeger et al., 1988; Cranford and Hill, 1999; Huang et al., 2002), it is clear that future models must increasingly account for these "alternative" food sources. The biochemical composition of DETORG and corresponding EDET are so variable (Héral et al., 1983) (Fig. 4), that unsubstantiated assumptions may lead to very significant error. In the present case, it should not be surprising that present simulations based upon POC were generally similar to those based upon POM (Figs. 5–7). This was because the average value of 6.1 J mg^{-1} for EDET as determined using POC was assumed in simulations based upon POM alone (refer to Methods).

Notable novel elements within our model include resolving significant adjustments in the relative processing of living chlorophyll-rich phytoplankton organics, non-phytoplankton organics and the remaining inorganic matter during both differential retention on the gill and selective pre-ingestive rejection within pseudofaeces. We have defined and used a relation whereby the filtration of PHYORG (FRPHYORG; mg h^{-1}) increased in linear relation with its abundance, but at rates that varied in coincident unimodal relation with POM ($p < 0.000001$) (refer to Methods). Alternatively, filtration rates for remaining non-phytoplankton organics (FRDETORG; mg h^{-1}) and PIM (FRPIM; mg l^{-1}) each increased in single positive relations with their availabilities (refer to Methods). These relations establish and simulate how efficiencies with which PHYORG was retained on the gills changed in response to differences in the relative composition of POM, whereas selective retentions of DETORG and PIM remained relatively constant. The above findings are consistent with recent observations in the mussel *Perna canaliculus*, in which retention efficiencies for PHYORG varied in similar unimodal relation with the proportion that PHYORG comprised of POM (Hawkins et al., 1999). For any given availability of PHYORG, maximal FRPHYORG occurred at only 2.6 mg l^{-1} of POM (refer to Methods), which was available at concentrations that averaged up to about 15 mg l^{-1} in Sungo Bay (Fig. 3). As previously discussed by Hawkins et al. (2001), such unimodal responses in feeding rate, with maxima that occur towards the lower extreme of naturally occurring concentrations, help to reconcile apparently conflicting differences in bivalve suspension-feeding behaviour. They also emphasize the importance of defining relations at low food availabilities, when responsive adjustments are of greatest physiological and ecological consequence.

Just as for selective retention during filtration, we have defined and used a novel relation that simulates preferential retention of PHYORG during selective processes associated with the production of pseudofaeces prior to ingestion. Here, the proportion of filtered PHYORG that was rejected in pseudofaeces (RRFRPHYORG; fraction) varied in inverse relation with the proportion of phytoplankton organics within filtered POM (PHYCNFPOM; mg mg − 1) ($p < 0.000001$) (refer to Methods). This shows that the efficiency with which PHYORG was selectively ingested increased with the relative abundance of PHYORG among all filtered organics. Again, single positive relations indicate that DETORG and PIM were rejected with relatively constant efficiencies (refer to Methods).

Certain functional relations observed in *C. farreri*, such as (i) unimodal responses in clearance and filtration rates to availability of CHL or PHYORG and (ii) inverse relations between net absorption efficiency (NAEIO; fraction) and the organic content of ingested organics (OCI; fraction) are common to other species of filter-feeding bivalve shellfish (Hawkins et al., 1998a,b, 1999). On this basis, we believe that a generic model structure can ultimately emerge for application in different species. Understandably, standardized comparisons using these relations are establishing subtle yet significant differences between the responsive behaviour of separate species (e.g. Hawkins et al., 1998a; Yukihira et al., 1998). Therefore, that generic model structure will need to accommodate all potential responses as evidenced between species. In the present circumstances, reproductive effort is consistently very low during the 2 years of culture, when chemical entrainment through the release of hormones in any case ensures that reproduction occurs over the same few days throughout Sungo Bay (refer to Methods). Therefore, we were able to explicitly represent

the timing and amount of spawning, rather than simulating these events by stipulating different priorities of energy allocation (e.g. Scholten and Smaal, 1999; Pouvreau et al., 2000b; Ren and Ross, 2001); nor was it necessary to consider effects of variable salinity, which was very stable, averaging (± 95% CL) 31.9 ± 0.1 ‰ for all measures throughout the year and bay. Relations in the present model were established over experimental ranges of TPM from 3 to 105 mg l^{-1}, POM from 0.5 to 13.6 mg l^{-1}, CHL from 0.8 to 151 μg l^{-1} and TEMP from 1 to 28 °C (Hawkins et al., 2001; Zhang et al., submitted for publication). Those ranges spanned all seasonal observations throughout Sungo Bay (Fig. 2), contributing to the successful simulation of observed growth. However, in applying dynamic models of this type to different environments, it is important to bear in mind that fitted relations may only be valid over the conditions under which they were measured. For example, relations used in the present model do not define the reduced feeding and growth that may ultimately result from the clogging of gills at higher seston loads (i.e. Barillé et. al., 1997a). If we wish to simulate growth in more turbid waters, it will be necessary to recalibrate and validate the model under those circumstances.

In summary, our model predicts the effects of main environmental drivers through a functional set of responsive interrelations. Notable novel elements include resolving significant adjustments in the relative processing of living chlorophyll-rich phytoplankton organics, non-phytoplankton organics and the remaining inorganic matter during both differential retention on the gill and selective pre-ingestive rejection within pseudofaeces. Where data are available describing POC, we also include a facility to predict the energy content of non-phytoplankton organics, which appears very much more variable than for phytoplankton organics. Whether using that facility or assuming an average value, resolution of relative processing enables simulation of how the organic composition and energy content of ingested matter change in response to tidal, seasonal or spatial differences in food availability and composition. Dependent relations predict rates of energy absorption, energy expenditure and excretion. By these means, our model successfully simulates short-term adjustments in feeding, biodeposition, excretion and growth across ranges of relevant natural variability. This is an important advance when compared with simpler models that are unable to predict responsive adjustments in feeding and metabolism. Only by modelling the complex set of feedbacks, both positive and negative, whereby suspension-feeding shellfish interact with ecosystem processes, can one realistically hope to assess environmental capacities for culture (Dowd, 1997; Prins et al., 1998). In separate papers, we describe how the present simulation has been coupled with a hydrodynamic model to consider effects of culture density upon growth at the local farm scale (Bacher et al., submitted for publication), as well as within larger-scale two dimensional models that simulate how different scenarios of multi-species culture affect the total harvestable yield in Sungo Bay (Duarte et al., submitted for publication (a,b); Nunes et al., in press).

Acknowledgements

This work was funded in part by (i) a European Community INCO-DC project ERBIC18CT980291 entitled “Carrying capacity and impact of aquaculture on the

environment in Chinese bays" and (ii) a Core Strategic Research Project entitled "Scaling Biodiversity, and the consequences of change" of the Plymouth Marine Laboratory. We also thank (i) Mr. Li Hongyi, General Director of Xunshan Fishery Company, for making available accommodation and the experimental site, including cultured algae and laboratory equipment; (ii) Mr. Wang Lichao, Director of Rongcheng Fishery Research Institute, for coordinating interaction between the research team and local government; and (iii) Dr. Bob Clarke of Plymouth Marine Laboratory for valuable statistical guidance. **[SS]**

References

Arifin, Z., Bendell-Young, L.I., 1997. Feeding response and carbon assimilation by the blue mussel *Mytilus trossulus* exposed to environmentally relevant seston matrices. Mar. Ecol., Prog. Ser. 160, 241–253.

Bacher, C., Duarte, P., Ferreira, J.G., Héral, M., Raillard, O., 1998. Assessment and comparison of the Marennes-Oléron Bay (France) and Carlingford Lough (Ireland) carrying capacity with ecosystem models. Aquat. Ecol. 31, 379–394.

Bacher, C., Grant, J., Hawkins, A.J.S., Fang, J., Zhu, M., Besnard, M., in press. Modelling the effect of food depletion on scallop growth in Sungo Bay (China). Aquatic Living Resources.

Baker, S.M., Levinton, J.S., Kurdziel, J.P., Shumway, S.E., 1998. Selective feeding and biodeposition by zebra mussels and their relation to changes in phytoplankton composition and seston load. J. Shellfish Res. 17, 1207–1213.

Barillé, L., Prou, J., Héral, M., Razet, D., 1997a. Effects of high natural seston concentrations on the feedings, selection, and absorption of the oyster *Crassostrea gigas* (Thunberg). J. Exp. Mar. Biol. Ecol. 212 (2), 149–172.

Barillé, L., Héral, M., Barillé-Boyer, A.-L., 1997b. Modélisation de l'écophysiologie de l'huître *Crassostrea gigas* dans un environnement estuarien. Aquat. Living Resour. 10, 31–48.

Bayne, B.L., Newell, R.C., 1983. Physiological energetics of marine molluscs. In: Wilbur, K.M., Saleuddin, A.S. (Eds.), The Mollusca, vol. 4. Academic Press, New York, pp. 407–515.

Beninger, P.G., Veniot, A., Poussart, Y., 1999. Principles of pseudofeces rejection on the bivalve mantle: integration in particle processing. Mar. Ecol., Prog. Ser. 178, 259–269.

Bougrier, S., Hawkins, A.J.S., Héral, M., 1997. Preingestive selection of different microalgal mixtures in *Crassostrea gigas* and *Mytilus edulis*, analysed by flow cytometry. Aquaculture 150, 123–134.

Brillant, M.G.S., MacDonald, B.A., 2000. Postingestive selection in the sea scallop, *Placopecten magellanicus* (Gmelin): the role of particle size and density. J. Exp. Mar. Biol. Ecol. 253, 211–227.

Brylinski, M., Sephton, T.W., 1991. Development of a computer simulation model of a cultured blue mussel (*Mytilus edulis*) population. Can. Tech. Rep. Fish. Aquat. Sci. 1805 (viii+81 pp.).

Cameron, C.J., Cameron, I.F., Paterson, C.G., 1979. Contribution of organic shell matter to biomass estimates of unionid bivalves. Can. J. Zool. 57, 1666–1669.

Campbell, D.E., Newell, C.R., 1998. MUSMOD, a production model for bottom culture of the blue mussel, *Mytilus edulis* L. J. Exp. Mar. Biol. Ecol. 219, 171–203.

Cranford, P.J., Hargrave, B.T., 1994. In situ time-series measurement of ingestion and absorption rates of suspension-feeding bivalves: *Placopecten magellanicus*. Limnol. Oceanogr. 39, 730–738.

Cranford, P.J., Hill, P.S., 1999. Seasonal variation in food utilisatization by the suspension-feeding bivalve molluscs *Mytilus edulis* and *Placopecten magellanicus*. Mar. Ecol., Prog. Ser. 190, 223–239.

Dowd, M., 1997. On predicting the growth of cultured bivalves. Ecol. Model. 104, 113–131.

Duarte, P., Meneses, R., Hawkins, A.J.S., Zhu, M., Fang, J., submitted for publication (a). Mathematical modelling to assess the carrying capacity for multi-species culture within coastal waters: I. Model development and implementation.

Duarte, P., Hawkins, A.J.S., Meneses, R., Fang, J., Zhu, M., submitted for publication (b). Mathematical

modelling to assess the carrying capacity for multi-species culture within coastal waters: II. Model application for bivalve culture optimisation.

Dupuy, C., Vaquer, A., Lam-Hoai, T., Rougier, C., Mazouni, N., Lautier, J., Collos, Y., Le Gall, S., 2000. Feeding rate of the oyster *Crassostrea gigas* in a natural planktonic community of the Mediterranean Thau Lagoon. Mar. Ecol., Prog. Ser. 205, 171–184.

Elliot, J.M., Davison, W., 1975. Energy equivalents of oxygen consumption in animal energetics. Oecologia 19, 195–201.

Epp, J., Bricelj, V.M., Malouf, R.E., 1988. Seasonal partitioning and utilisation of energy reserves in two age classes of the bay scallop *Argopecten irradians* (Lamarck). J. Exp. Mar. Biol. Ecol. 121, 113–136.

Fang, J., Sun, H., Kuang, S., Sun, Y., Zhou, S., Song, Y., Cui, Y., Zhao, J., Yang, Q., Li, F., Grant, J., Emerson, C., Wang, X., Tang, T., 1996. Study on the carrying capacity of Sanggou Bay for the culture of scallop *Chlamys farreri*. Mar. Fish. Res. 17, 18–31.

Fegley, S.R., MacDonald, B.A., Jacobsen, T.R., 1992. Short-term variation in the quantity and quality of seston available to benthic suspension feeders. Estuar. Coast. Shelf Sci. 34, 393–412.

Ferreira, J.G., Duarte, P., Ball, B., 1998. Trophic capacity of Carlingford Lough for oyster culture-analysis by ecological modelling. Aquat. Ecol. 31, 361–378.

Gnaiger, E., 1983. Calculation of energetic and biochemical equivalents of respiratory oxygen consumption. In: Gnaiger, E., Forstner, H. (Eds.), Polarographic Oxygen Sensors: Aquatic and Physiological Applications. Springer Verlag, Berlin, pp. 337–345.

Grant, J., Bacher, C., 1998. Comparative models of mussel bioenergetics and their validation at field culture sites. J. Exp. Mar. Biol. Ecol. 219, 21–44.

Guo, X., Ford, S., Zhang, F., 1999. Molluscan aquaculture in China. J. Shellfish Res. 18, 19–32.

Hawkins, A.J.S., Widdows, J., Bayne, B.L., 1989. The relevance of whole-body protein metabolism to measured costs of maintenance and growth in *Mytilus edulis*. Physiol. Zool. 62, 745–763.

Hawkins, A.J.S., Smith, R.F.M., Bayne, B.L., Héral, M., 1996. Novel observations underlying fast growth of suspension-feeding shellfish in turbid environments: *Mytilus edulis*. Mar. Ecol., Prog. Ser. 131, 179–190.

Hawkins, A.J.S., Smith, R.F.M., Tan, S.H., Yasin, Z.B., 1998a. Suspension-feeding behaviour in tropical bivalve molluscs: *Perna viridis*, *Crassostrea belcheri*, *Crassostrea iradelei*, *Saccostrea cucculata* and *Pinctada margarifera*. Mar. Ecol., Prog. Ser. 166, 173–185.

Hawkins, A.J.S., Bayne, B.L., Bougrier, S., Héral, M., Iglesias, J.I.P., Navarro, E., Smith, R.F.M., Urrutia, M.B., 1998b. Some general relationships in comparing the feeding physiology of suspension-feeding bivalve molluscs. J. Exp. Mar. Biol. Ecol. 219, 87–103.

Hawkins, A.J.S., James, M.R., Hickman, R.W., Hatton, S., Weatherhead, M., 1999. Modelling of suspension-feeding and growth in the green-lipped mussel *Perna canaliculus* exposed to natural and experimental variations of seston availability in the Marlborough Sounds, New Zealand. Mar. Ecol., Prog. Ser. 191, 217–232.

Hawkins, A.J.S., Fang, J.G., Pascoe, P.L., Zhang, J.H., Zhang, X.L., Zhu, M.Y., 2001. Modelling short-term responsive adjustments in particle clearance rate among bivalve suspension-feeders: separate unimodal effects of seston volume and composition in the scallop *Chlamys farreri*. J. Exp. Mar. Biol. Ecol. 262, 61–73.

Héral, M., Deslous-Paoli, J.M., Sornin, J.M., 1983. Transferts énergétics entre l'huître *Crassostrea gigas* et la nourriture potentielle disponible dans un bassin ostréicole: premières approches. Oceanis 9, 169–194.

Holm-Hansen, O., Lorenzen, C.J., Holmes, R.W., Strickland, J.D.H., 1965. Fluorometric determination of chlorophyll. J. Cons.-Cons. Int. Explor. Mer 30, 3–15.

Huang, S.C., Kreeger, D., Newell, R.I.E., 2002. Seston available as a food resource for the ribbed mussel (*Geukensia demissa*) in a North-American, Mid-Atlantic saltmarsh. Estuar. Coast. Shelf Sci. 56.

James, M.R., Ross, A.H., 1997. Sustainability—how many mussels can we farm? Aquac. Update 18, 1–4.

Jørgensen, C.B., 1996. Bivalve filter feeding revisited. Mar. Ecol., Prog. Ser. 142, 287–302.

Kreeger, D.A., Langdon, C.J., Newell, R.I.E., 1988. Utilization of refractory cellulosic carbon derived from Spartina alterniflora by the ribbed mussel *Geukensia demissa*. Mar. Ecol., Prog. Ser. 42, 171–179.

Loret, P., Pastoureaud, A., Bacher, C., Delesalle, B., 2000. Phytoplankton composition and selective feeding of the pearl oyster *Pinctada margaritifera* in the Takapoto lagoon (Tuamotu Archipelago, French Polynesia): in situ study using optical microscopy and HPLC pigment analysis. Mar. Ecol., Prog. Ser. 199, 55–67.

Lou, Y., 1991. China. In: Shumway, S.E. (Ed.), Scallops: Biology, Ecology and Aquaculture. Elsevier, New York, pp. 809–824.

Lu, R., Ji, R., Zou, Y., Xia, B., Li, R., Zhu, M., 2000. A study on the feeding of three bivalves. Acta Oceanol. Sin. 22, 306–312.

MacDonald, B.A., Thompsin, R.J., Bourne, N.F., 1991. Growth and reproductive energetics of three scallop species from British Columbia (*Chlamys hastata*, *Chlamys rubiba*, and *Crassadoma gigantea*). Can. J. Fish. Aquat. Sci. 48, 215–221.

Møhlenberg, F., Riisgård, H.U., 1978. Efficiency of particle retention in 13 species of suspension-feeding bivalves. Ophelia 17, 239–246.

Nunes, J.P., Ferreira, J.G., Gazeau, F., Lencart-Silva, J., Zhang, X.L, Zhu, M.Y., Fang, J.G., in press. A model for sustainable management of shellfish polyculture in coastal bays. Aquaculture.

Platt, T., Irwin, B., 1973. Caloric content of phytoplankton. Limnol. Oceanogr. 18, 306–309.

Pouvreau, S., Bodoy, A., Buestel, D., 2000a. In situ suspension feeding behaviour of the pearl oyster *Pinctada margaritifera*: combined effects of body size and weather-related seston composition. Aquaculture 181, 91–113.

Pouvreau, S., Bacher, C., Héral, M., 2000b. Ecophysiological model of growth and reproduction of the black pearl oyster, *Pinctada margaritifera*: potential applications for pearl farming in French Polynesia. Aquaculture 186, 117–144.

Powell, E.N., Hofmann, E.E., Klinck, J.M., Ray, S.M., 1992. Modelling oyster populations: I. A commentary on filtration rate. Is faster always better? J. Shellfish Res. 11, 387–398.

Price, T.J., Thayer, G.W., LaCroix, M.W., Montgomery, G.P., 1976. The organic content of shells and soft tissues of selected estuarine gastropods and pelecypods. Proc. Natl. Shellfish. Ass. 65, 26–31.

Prins, T.C., Smaal, A.C., Dame, R.F., 1998. A review of the feedbacks between bivalve grazing and ecosystem processes. Aquat. Ecol. 31, 349–359.

Raillard, O., Menésguen, A., 1994. An ecosystem box model for estimating the carrying capacity of a macrotidal shellfish system. Mar. Ecol., Prog. Ser. 115, 117–130.

Raillard, O., Deslous-Paoli, J.M., Héral, M., Razet, D., 1993. Modélisation du comportement nutritionnel et de la croissance de l'huître japonaise *Crassostrea gigas*. Oceanol. Acta 16, 73–82.

Ren, J.S., Ross, A.H., 2001. A dynamic energy budget model of the Pacific oyster *Crassostrea gigas*. Ecol. Model. 142, 105–120.

Ren, J.S., Ross, A.H., Schiel, D.R., 2000. Functional descriptions of feeding and energetics of the Pacific oyster *Crassostrea gigas* in New Zealand. Mar. Ecol., Prog. Ser. 208, 119–130.

Ross, A.H., Nisbet, R.M., 1990. Dynamic models of growth and reproduction of the mussel *Mytilus edulis* L. Funct. Ecol. 4, 777–787.

Scholten, H., Smaal, A.C., 1999. The ecophysiological response of mussels (*Mytilus edulis*) in mesocosms to a range of inorganic loads: simulations with the model EMMY. Aquat. Ecol. 33, 83–100.

Shumway, S.E., Cucci, T.L., Newell, R.C., Yentch, T.M., 1985. Particle selection, ingestion and absorption in filter-feeding bivalves. J. Exp. Mar. Biol. Ecol. 91, 77–92.

Shumway, S.E., Cucci, T.L., Lesser, M.P., Bourne, N., Bunting, B., 1991. Particle selection by three species of scallops. J. Shellfish Res. 10, 273.

Slobodkin, L.B., Richman, S., 1961. Calories/gm in species of animals. Nature 191, 299.

Smaal, A.C., Verhagen, J.H.G., Coosen, J., Haas, H.A., 1986. Interaction between seston quantity and quality and benthic suspension feeders in the Oosterschelde, The Netherlands. Ophelia 26, 385–399.

Soletchnik, P., Goulletquer, P., Héral, M., Razet, D., Geairon, P., 1996. Évaluation du bilan énergétique de l'huître creuse, *Crassostrea gigas*, en baie de Marennes-Oléron (France). Aquat. Living Resour. 9, 65–73.

Solidoro, C., Pastres, R., Melaku Canu, D., Pellizzato, M., Rossi, R., 2000. Modelling the growth of *Tapes philippinarum* in North Adriatic lagoons. Mar. Ecol., Prog. Ser. 199, 137–148.

Taylor, A.H., Geider, R.J., Gilbert, F.J.H., 1997. Seasonal and latitudinal dependencies of phytoplankton carbon-to-chlorophyll *a* ratios: results of a modelling study. Mar. Ecol., Prog. Ser. 152, 51–66.

Urrutia, M.B., Navarro, E., Ibarrola, I., Iglesias, J.I.P., 2001. Preingestive selection processes in the cockle *Cerastoderma edule*: mucus production related to rejection of pseudofaeces. Mar. Ecol., Prog. Ser. 209, 177–187.

Van Haren, R.J.F., Kooijman, S.A.L.M., 1993. Application of a dynamic energy budget model to *Mytilus edulis* (L.). Neth. J. Sea Res. 31, 119–133.

Ward, J.E., MacDonald, B.A., 1996. Pre-ingestive feeding behaviours of two sub-tropical bivalves (*Pinctada imbricata* and *Arca zebra*): responses to an acute increase in suspended sediment concentration. Bull. Mar. Sci. 59, 417–432.

Welschmeyer, N.A., Lorenzen, C.J., 1984. Carbon-14 labeling of phytoplankton carbon and chlorophyll *a* carbon: determination of specific growth rates. Limnol. Oceanogr. 29, 135–145.

Widdows, J., 1973. Effect of temperature and food on the heart beat, ventilation rate and oxygen uptake of *Mytilus edulis*. Mar. Biol. 20, 269–276.

Widdows, J., 1978. Physiological indices of stress in *Mytilus edulis*. Mar. Biol. Assoc. UK 58, 125–142.

Widdows, J., Hawkins, A.J.S., 1989. Partitioning of rate of heat dissipation by *Mytilus edulis* into maintenance, feeding and growth components. Physiol. Zool. 62, 764–784.

Williams, P., 1981. Detritus utilisation by *Mytilus edulis*. Estuar. Coast. Shelf Sci. 12, 739–746.

Wong, W.H., Cheung, S.G., 2001. Feeding rhythms of the green-lipped mussel, *Perna viridis* (Linnaeus, 1758) (Bivalvia: Mytilidae) during spring and neap tidal cycles. J. Exp. Mar. Biol. Ecol. 257, 13–36.

Yukihira, H., Klumpp, D.W., Lucas, J.S., 1998. Comparative effects of microalgal species and food concentration on suspension feeding and energy budgets of the pearl oysters *Pinctada margaritifera* and *P. maxima* (Bivalvia: Pteriidae). Mar. Ecol., Prog. Ser. 171, 71–84.

Zhang, F.S., Yang, H.S., 1999. Analysis of the causes of mass mortality of farming *Chlamys farreri* in summer in coastal areas of Shandong, China. Mar. Sci. (China) 1, 44–47.

Zhang, J., Fang, J.G., Hawkins, A.J.S., Pascoe, P.L., submitted for publication. Influence of temperature on clearance and oxygen consumption rates in the scallop *Chlamys farreri*.